Study of biological properties of gold nanoparticles: low toxicity, no proliferative activity, no ability to induce cell gene expression and no antiviral activity

Beatriz Salesa[1], Patricia Ferrús-Manzano[1], Alberto Tuñón-Molina[1], Alba Cano-Vicent[1], Marcelo Assis[2], Juan Andrés[2] and Ángel Serrano-Aroca[1,*]

[1] Biomaterials and Bioengineering Lab, Centro de Investigación Traslacional San Alberto Magno, Universidad Católica de Valencia San Vicente Mártir, c/Guillem de Castro 94, 46001 Valencia, Valencia, Spain.
[2] Department of Physical and Analytical Chemistry, University Jaume I (UJI), 12071 Castellon, Spain

*Corresponding author: angel.serrano@ucv.es (Á.SA)

Abstract

Gold nanoparticles (AuNPs) are a fundamental building block of many applications across nanotechnology as they have excellent biosafety which make them promising for a broad range of biomedical applications. Here we explore their *in vivo* toxicity, cytotoxicity and proliferative capacity in human keratinocyte HaCaT cells, their ability to induce gene expression and their antiviral properties against a surrogate of SARS-CoV-2. These nanoparticles were characterized by transmission electron microscopy, dynamic light scattering and zeta potential. The results showed that these AuNPs with sizes ranging from 10 to 60 nm are non-toxic *in vivo* at any concentration up to 800 µg/mL. However, AuNP cytotoxicity in human HaCaT cells is time-dependent, so that concentrations of up to 300 µg/mL did not show any *in vitro* toxic effect at 3, 12 and 24 h, although higher concentrations were found to have some significant toxic activity, especially at 24 h. No significant proliferative activity was observed when using low AuNP concentrations (10, 20 and 40 µg/mL), while the AuNP antiviral tests indicated low or insignificant antiviral activity. Surprisingly, none of the 13 analyzed genes had their expressions modified after 24 h's exposure to AuNPs. Therefore, the results show that AuNPs are highly stable inactive materials and thus very promising for biomedical and clinical applications demanding this type of materials.

Keywords: gold nanoparticles; human keratinocytes; proliferation; gene expression; cytotoxicity.

1. Introduction

Gold nanoparticles (AuNPs) are the subject of ever-growing interest in the field of nanotechnology due to their versatility and tunability in terms of size, morphology, surface chemistry and other properties [1,2]. They have also been recognized for their biocompatibility for health-related applications [3].

AuNPs are now being used in drug-delivery systems, cancer therapy, catalysis, chemical sensing, cosmetics, biomedicine, food products and many more applications [4–7]. They are inert, possess low or none toxicity and can be made stable in a range of solvents and pH values, desirable features from a biological standpoint [8–10].

Today AuNPs can be synthesized reproducibly and modified with seemingly limitless chemical functional groups [11].

AuNPs have excellent antibacterial efficacy alone against Enteric Bacterial Human Pathogen [12] or in combination with *panchagavya*, mainly against Gram-negative bacteria such as *Escherichia coli* or *Klebsiella pneumoniae* and against Gram-positive *Bacillus subtilis*[13]. However, other studies have shown that AuNPs are generally not bactericidal [14].

Advanced antimicrobial agents based on AuNPs can be produced combining these metal nanomaterials with antibiotics [14] or with antimicrobial peptides [15].

AuNPs have shown also antiviral effect against the influenza virus [16] and anticancer properties against glioblastoma cells [17]. The antiviral activity of nonfunctionalized AuNPs against herpes simplex virus type-1 was revealed in another study[18].

However, Rainer Haag and his collaborators have also found that the antiviral effect of AuNPs is highly dependent on their sizes [19].

Delivery of antiviral small interfering RNA has been performed with AuNPs to successfully inhibit dengue virus infection [20].

This paper outlines our achievements with AuNPs in several biological properties that have not been tested before such as proliferative activity of human keratinocyte HaCaT cells and their ability to induce cell gene expression of a wide range of genes (*SOD1, CAT, MMP1, TGFB1, GPX1, FN1, HAS2, LAMB1, LUM, CDH1, COL4A1, FBN* and *VCAN*). These 13 genes are involved in different metabolic routes which are very relevant for biomedical applications such as oxidative stress, extracellular matrix, synthesis of proteins related to the maintenance and repair of different tissues.

We explore also their cytotoxicity and *in vivo* toxicity using the *Caenorhabditis elegans* model for the first time.

Finally, the antiviral properties of AuNPs are study against bacteriophage phi6. This bacteriophage is an enveloped double-stranded RNA virus[21] that is a biosafe model of enveloped viruses such as SARS-CoV-2, Influenza or Ebola [22,23].

The AuNPs used in this study are characterized by transmission electron microscopy, dynamic light scattering (DLS) to evaluate their particle hydrodynamic size in water solution and in Dulbecco's modified Eagle medium (DMEM), used for the biological characterization, and zeta potential in water as a function of pH.

2. Materials and Methods

2.1. Materials

Gold nanopowder (< 100 nm particle size, Product Code 636347, 99.9% trace metals basis) were purchased from Sigma-Aldrich (Switzerland). Fetal bovine serum (FBS), DMEM low glucose, peniciline-streptomicine (P/S), L-glutamine and Epidermal Growth Factor (EGF) were obtained from Life Technologies (Gibco, Karlsruhe, Germany), MTT reagent from Sigma-Aldrich (Switzerland), RNA purification kit from Norgen (Canada), and PrimeScript™ RT Reagent Kit (Perfect Real Time) from Takara Bio Inc. Bacteriological agar, tryptic soy broth (TSB) and tryptic soy agar (TSA) from Scharlau (Ferrosa, Barcelona, Spain).

2.2. Material characterization

Transmission electron microscopy (TEM) was performed with JEL 2100 (Tokyo, Japan) equipment with a LaB_6 thermoionic gun operated at 200 kV. The sample was prepared in aqueous solution dropped onto a copper grid. The zeta potential (ζ) of the AuNPs was analyzed in water solutions as a function of pH. The zeta potential (ζ), DLS, and polydispersity index (PdI) values were obtained from a Zetasizer NanoZS (Malvern, United Kingdon). For the ζ measurements, pH was adjusted with solutions of NH_4OH (Synth, 24%) and HNO_3 (Synth, 70%). The dynamic light scattering (DLS) technique was used to evaluate the particle hydrodynamic size of the AuNPs in water solution and in DMEM, used for the biological characterization.

2.3. Culture manteinance

HaCaT, an immortalized human keratinocytes cell line provided by La Fe Health Research Institute (Valencia, Spain), was used to perform the in vitro assays. The culture stock was maintained in an incubator in a humidified atmosphere at 5 % CO^2 and 37 ºC. A culture medium was used for growth based on DMEM low glucose, supplemented with FBS 10 %, L-glutamine 2% and P/S 1 %. The medium was renewed three times per week and cells were maintained under 80 % confluence in the flask culture.

2.4. Preparation of nanoparticle stock solution

To prepare gold nanoparticle stock solutions for the experimental assays, they were resuspended in the same medium used for the stock culture but without FBS. The mixes were sonicated for 2 hours at room temperature to obtain a homogeneous solution. A medium vial without nanoparticles was also exposed to the same conditions as the homogenates to ensure that any possible changes due to sonication did not affect its integrity, as it would later be used as the medium for the control groups. All the sonicated solutions were used immediately after the end of this process.

2.5. Cytotoxicity Assay

2.5.1 In vitro cytotoxicity

AuNPs cytotoxicity was evaluated through 3-(4, 5-dimethylthiazol-2-yl)-2, 5-diphenyl tetrazolium (MTT) assay. HaCaT cells were detached from the culture flask, and counted for seeding in 96-well plates at a density of 1 x 10^4 cells per well. After growing for 24 hours in the incubator (same conditions as cell culture stock) the medium was replaced with 100 uL of each experimental solution plus a control group. Each

AuNPs concentration was tested in sextuplicate for three different periods of time in order to evaluate the different 3, 12 and 24 hour endpoints. The range concentration selected to calculate the EC_{50} at 3 hours was 40, 80, 150, 300, 500 to 800 µg/mL, and 0, 40, 80, 150, 300, 500 and 800 µg/mL at 12 and 24 h. The medium was removed after the different incubation periods, the cells were washed with PBS 1x and MTT reagent was added to each well for 5 hours. The MTT reagent was then replaced by DMSO to solubilyze formazan crystals and absorbance was measured by a Varioskan multiwell plate reader (ThermoScientific, Canada) at 550 nm.

2.5.2 In vivo cytotoxicity

In vivo toxicity was examined in the *C. elegans* model. AuNP solutions were prepared at double the concentration tested in potassium medium (K medium) (2.36 g potassium chloride, 3 g sodium chloride in 1 L distilled water, autoclaved). The worms were preserved and disseminated on OP50 E. coli seeded nematode growth medium (NGM) made according to Stiernagle, T.(Stiernagle, 2006) at 25 °C. An N2 strain was used for these assays provided by the Caenorhabditis Genetics Center (CGC, Minneapolis, MN, USA). The worms and eggs were cleaned off NGM plates using 5 mL of distilled water and concentrated in 15 mL falcon tubes to form an L1 stage-synchronized C. elegans population. The tubes were centrifuged at 1300 r.p.m. (2209× g) for 3 min and the supernatant was discarded. The *C. elegans* pellet was resuspended in 100 µL of dH_2O and displaced to Eppendorf tubes, adding 700 µL of a 5% bleaching solution. This suspension was incubated for 15 min and vortexed every 2 min. Subsequent to the final vortexing, the Eppendorf tubes were centrifuged at 700× g for 3 min. the supernatant was discarded and the pellet was washed in 800 µL of dH_2O. This step was carried out two extra times. After the final washing step, the pellet was resuspended in 100 µL of dH_2O and displaced to NGM plates supplied with 100 µL of an OP50 E. coli culture. The eggs were hatched for 72 h at 25 °C. Centrifugation at 1300 r.p.m. (2209× g) for 3 min was performed to pellet the L1 staged worms, and resuspended in 3 mL of potassium medium. A 48-well plate was used to prepare the wells, including 62.5 µL of a 1:250 suspension of cholesterol (5 mg/mL in ethyl alcohol) in a sterile potassium medium, 62.5 µL of a 50× concentrated OP50 E. coli culture at OD_{600} of 0.9, pelleted by centrifugation at 4000 r.p.m. (6797× g) for 10 min and resuspended in a potassium medium, 115 µL of potassium medium and 250 µL of the corresponding AuNPs solution. A volume of K medium containing 50–100 worms was then mixed in the wells. The 48-well plates were closed up with parafilm and placed in an orbital shaker at 25 °C and 120 r.p.m. for 24 h. With a view to determining the lifespan of C. elegans, the amount of liquid in each well was distributed in 10 drops of 50 µL and placed under a microscope (Motic BA410E including Moticam 580 5.0MP) to calculate the amount of living and dead C. elegans. Positive and negative control were development in the K medium and bleach, respectively. Growth was evaluated in heat-killed portions by measuring the body length in an image taken under the microscope on Motic Images Plus 3.0 software. Five independent replicates (n = 5) were managed for this assay.

2.6. Proliferation Assay

To conduct this test, the cells were also seeded in 96-well plates but at a density of 5×10^3 cells per well. AuNP solutions were prepared following the protocol described above but in this case with FBS 0.5 %, including the control media. 2 non-cytotoxic

concentrations were selected according to the cytotoxic results at 24 h. The cells were cultured at each experimental concentration for 72 hours, after which the MTT assay was performed to evaluate cell growth. A positive proliferation control was also included in each plate, exposed to epidermal growth factor (EGF) at a concentration of 15 ng/mL. Each experimental condition was tested in sextuplicate.

2.7. Gene expression

For the gene expression studies, the cells were seeded in 6-well culture plates at a density of 1.5 x 10^6 cells per well. As in the proliferation assays, two non-cytotoxic concentrations were selected based on the previously obtained results. The cells were incubated for 24 h with each experimental solution (preparation as described above) and RNA was extracted by using an RNA purification kit (Norgen, Canada). After determining the concentration and quality of the extracted RNA by a Nanodrop One (ThermoFisher, Canada), cDNA synthesis and RT-qPCR were performed. For data analysis the QuantStudio™ Design & Analysis Software" (ThermoFisher, Canada) was used. The primer design for each target gene (Table A1 in Appendix A published previously in reference[24]) and reference gene (β-actin/ACTB) was designed on Primer-Blast software (available on: http://www.ncbi.nlm.nih.gov/tools/primer-blast). The data were normalized and analyzed according to the expression of the reference gene.

2.8. Antiviral test

A well-know antiviral compound such as benzalkonium chloride [25,26] was always used in the experiments as a positive control. AuNP stock solutions were prepared in sterile tryptic soy broth (TSB, Scharlau), sonicated for 2 h at maximum power to homogenize the solution and was used immediately after sonication. A vial containing TSB was also exposed to the same conditions and then used with the control groups and for the preparation of the different stock concentrations.

Pseudomonas syringae (DSM 21482) and bacteriophage phi 6 (DSM 21518) were purchased from the Leibniz Institute DSMZ-German Collection of Microorganisms and Cell Cultures GmbH (Braunschweig, Germany). This Gram-negative bacterium was cultured in solid tryptic soy agar (TSA, Scharlau) and subsequently in liquid TSB at 120 r.p.m. and a temperature of 25ºC. Bacteriophage phi 6 propagation was carried out according to the Leibniz Institute DSMZ-German Collection of Microorganisms and Cell Cultures GmbH specifications. The antiviral assay was performed at a dispersion of 50 µL of TSB with phages placed at a titer of approximately 1x10^6 plaque forming units per mL (PFU/mL) onto 50 µl of each different AuNP concentrations. These suspensions were incubated for 24h at 25ºC and 240 r.p.m.. The different suspensions were individually placed in falcon tubes with a TSB volume of 10 mL to be sonicated at 25ºC for 5 min, followed by 1 min of vortexing. Serial dilutions were performed from each falcon tube for bacteriophage titration, after which 100 µL of each phage dilution was mixed with 100 µL of the bacterial host at $OD600_{nm}$ = 0.5. The bacteriophage infective capacity was thus studied according to the double-layer assay [27]. A volume of 4 mL of top agar (TSB + 0.75% bacteriological agar) from Scharlau (Ferrosa, Barcelona, Spain) with 1 mM calcium chloride and the bacteriophage/bacteria suspension were mixed and poured on TSA plates to be cultured at 25ºC in a temperature-controlled incubator for 24 h. Phage titers in PFU/mL of each sample were compared with the control, which consisted of 50 µL of phage added directly to the bacterial culture without being in contact with any AuNP solution and without the sonication/vortexing treatment. The antiviral activity of

the different AuNP concentrations was determined at 24 hours of contact with the bacteriophage phi 6 in log reductions of titers. It was ensured that the sonication/vortexing treatment did not affect the infectious activity of the bacteriophage phi 6 and that the residual disinfectants of the titrated samples did not interfere with the titration process. Three independent antiviral tests were performed on two different days (n = 6) to ensure reproducibility.

2.9. Statistical analysis

The results obtained in the study were statistically analyzed by ANOVA, followed by multiple Tukey's post-hoc analysis. Median effective concentration (EC_{50}) values were estimated by Probit analysis. The results were obtained on GraphPad Prism 6 software at a significance level of at least $p < 0.05$.

3. Results

3.1. Material characterization

High-resolution TEM (HR-TEM) images of the AuNPs are shown in Figure 1a-c at different magnifications.

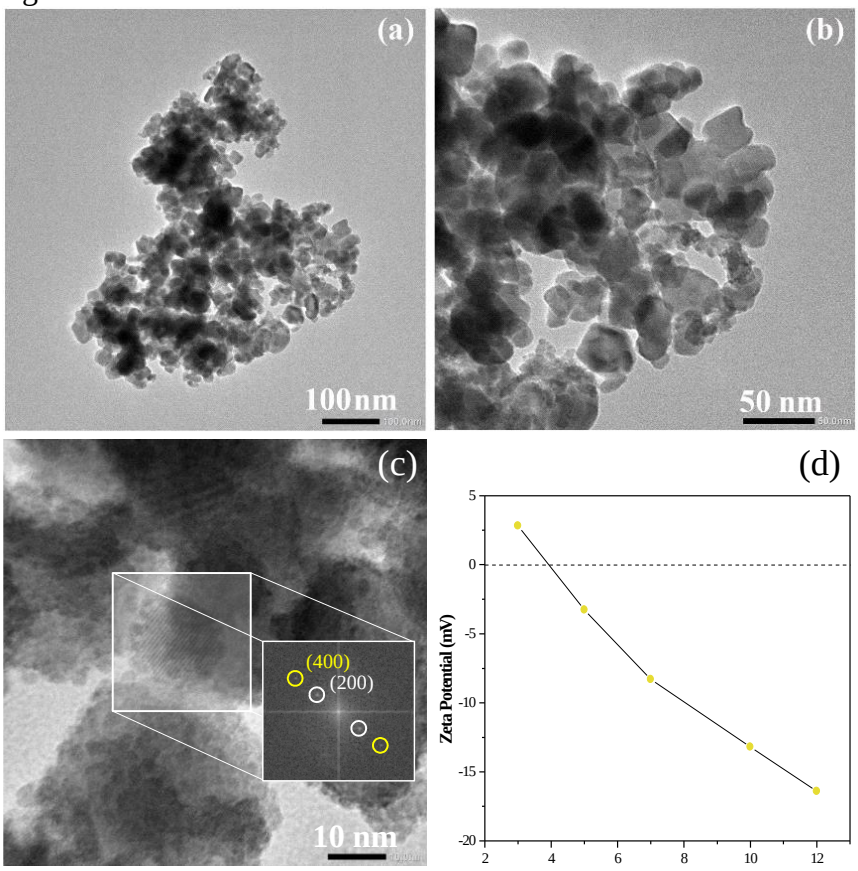

Figure 1. Transmission electron micrographs of gold nanoparticles at three different magnifications (a, b, c) and the zeta potential dependency of pH (d).

Figure 1d shows the zeta potential dependency of pH. The DLS technique shows the particle size values according to nanofluid preparation with water solution or DMEM in Table 1.

Table 1. Particle hydrodynamic sizes in nm of the gold nanoparticles in water solution and in the Dulbecco's modified Eagle medium (DMEM) used for the biological characterization determined by the dynamic light scattering technique. The polydispersity index (PdI) values of the gold nanoparticles (AuNPs) are also indicated

Material	DLS (nm)		PdI	
	Water	**DMEM**	**Water**	**DMEM**
AuNPs	339.9	781.6	0.369	0.579

3.2. Biological properties

The time-dependent cytotoxicity, proliferation and gene expression results determined for AuNPs, AgNPs, GNPs and CNFs in human keratinocytes HaCaT cells is described in the following subsections.

3.2.1. Cytotoxicity Assay

Figure 2 shows the concentration-dependence *in vitro* toxicity of AuNPs as a function of time (3, 12 and 24 h). The mean effective concentrations of HaCaT cells after treatment with AuNPs were calculated from these results and are shown in Table 2.

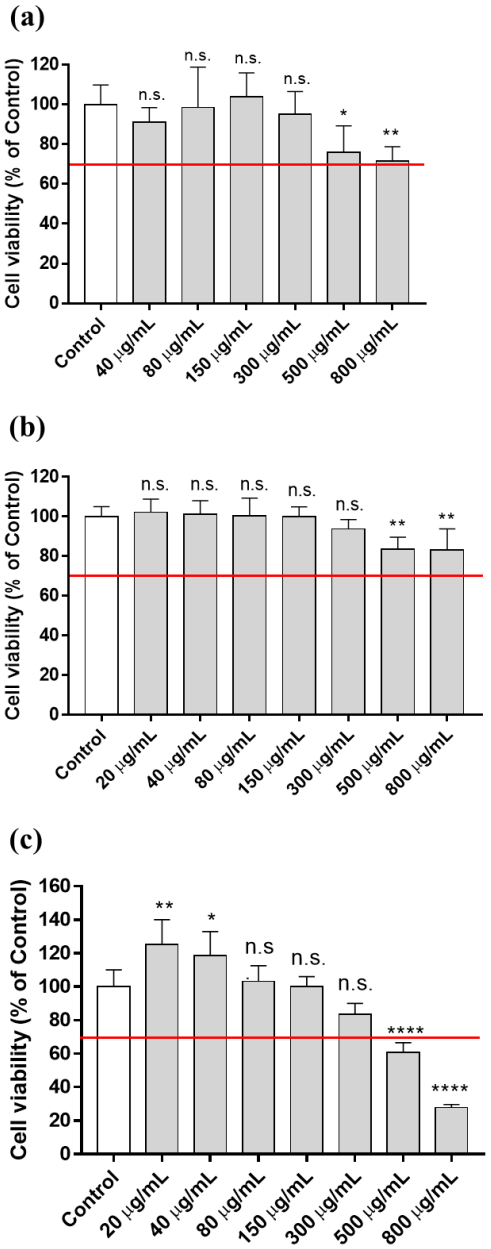

Figure 2. Cell viability in human keratinocyte (HaCaT) cells, after 3 (a), 12 (b) and 24 h (c) exposure to gold nanoparticles (AuNPs) at different concentrations ranging from 20 to 800 µg/mL. Cell viability was evaluated by the MTT assay. The results are represented as a percentage of the control group. Data are presented as the mean ± standard deviation of six replicates. The ANOVA results of the different GO concentrations with respect to control are indicated in the plot. * $p < 0.05$; ** $p < 0.01$; *** $p < 0.001$; **** $p < 0.0001$; n.s: not significant. The red line indicates the limit below which the sample is cytotoxic according to the ISO-10993 standard.

Table 2. Mean effective concentration (EC_{50}) of HaCaT cells after treatment with gold nanoparticles (AuNPs) at different exposure times (3, 12 and 12 hours). Mean EC_{50} and confidence limits 95% (CI) are shown as the mass-volume concentration, µg/mL. Goodness of fit (R square) is also indicated.

Exposure (h)	EC_{50} (µg/mL)	95% CI	R square
3	1264.7	964.9-2301.1	0.5348
12	975.6	652.4-2141.1	0.5113

24	573.8	539.5-611.1	0.9407

3.2.2. In vivo Cytotoxicity assay

Figure 3 gives the results of the *in vivo* toxicity assays using *C. elegans* after acute (24 hours) or chronic (72 hours) exposure: survival rate (%) and growth in length (%) .

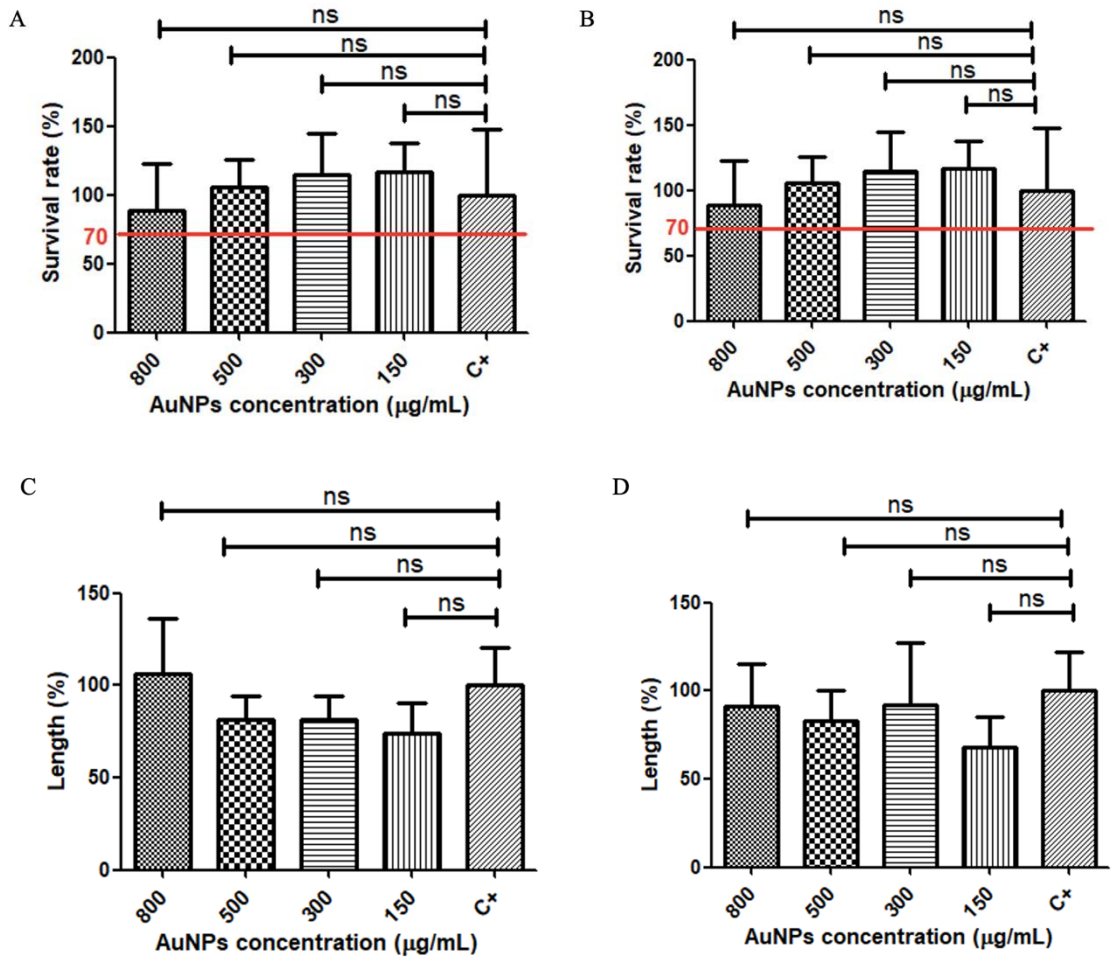

Figure 3. *In vivo* toxicity in *C. elegans* model: survival rate (%) after acute (24 h) exposure (A) and chronic (72 h) exposure (B) and growth in length (%) after acute (24 h) exposure (C) and chronic (72 h) exposure (D) to K medium positive control (C+), 150 µg/mL AuNPs in K medium (150), 300 µg/mL AuNPs in K medium (300), 500 µg/mL AuNPs in K medium (500), and 800 µg/mL AuNPs in K medium (800), with respect to the positive control (100%). Five independent replicates (n=5) were carried out. Results are shown as mean ± standard. Statistical analysis performed by one way ANOVA with Tukey's correction for multiple comparisons: ns, not significant. The red line indicates the limit below which the sample is cytotoxic according to the ISO-10993 standard.

3.2.2. Proliferation Assay

The proliferative effect of AuNPs in human keratinocytes is shown in Figure 4.

Figure 4. Proliferation in human keratinocytes stimulated by exposure to different gold nanoparticle (AuNPs) concentrations (10, 20 and 40 μg/mL) at 72 hours of exposure. Data are presented as the mean ± standard deviation (SD) of six replicates. The ANOVA results of the different AuNP concentrations and

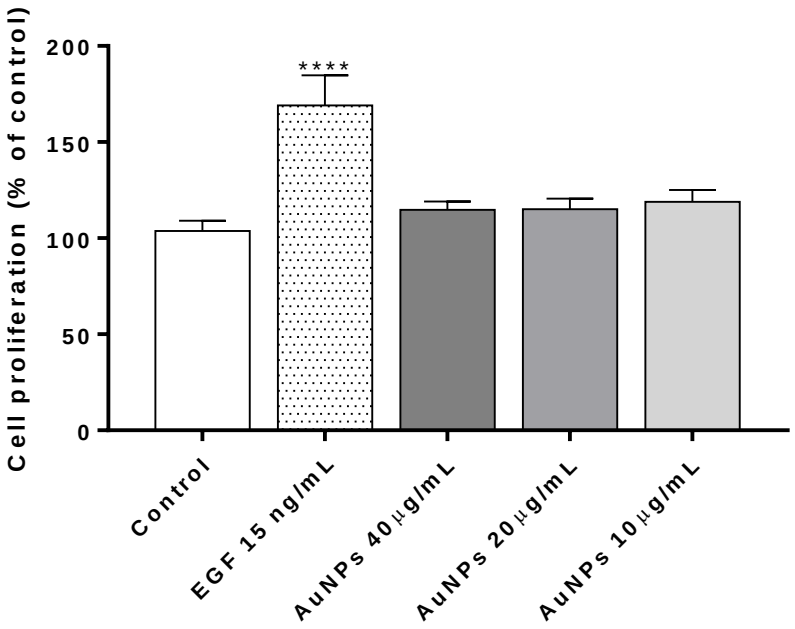

epidermal growth factor (EGF) with respect to control are indicated in the plot. * $p > 0.05$; ** $p > 0.01$; *** $p > 0.001$; n.s: not significant.

3.2.3. Gene expression

Figure 5 shows the effect of the AuNPs on the expression of 13 genes (*SOD1*, *CAT*, *MMP1*, *TGFB1*, *GPX1*, *FN1*, *HAS2*, *LAMB1*, *LUM*, *CDH1*, *COL4A1*, *FBN* and *VCAN*) at non-cytotoxic concentrations in human keratoncyte HaCaT cells after 24 hours.

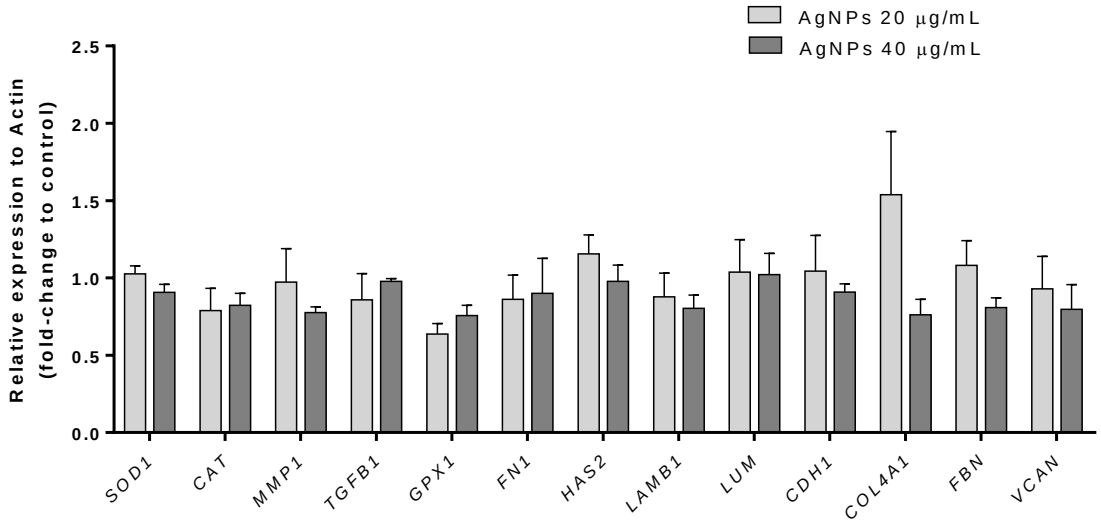

Figure 5. Effect of gold nanoparticles (AuNPs) on the expression of 13 genes (*SOD1, CAT, MMP1, TGFB1, GPX1, FN1, HAS2, LAMB1, LUM, CDH1, COL4A1, FBN and VCAN*) at non-cytotoxic concentrations (20 and 40 µg/mL) in the human keratinocyte HaCaT cell line after 24 hours. Data are presented as mean ± SD from three replicates. Results are given as fold-change of control and relative expression to ACTB.

3.2.4. Antiviral assay

AuNP antiviral properties were tested against bacteriophage phi 6, a surrogate virus of SARS-CoV-2 [23] (Figure 6 and 7).

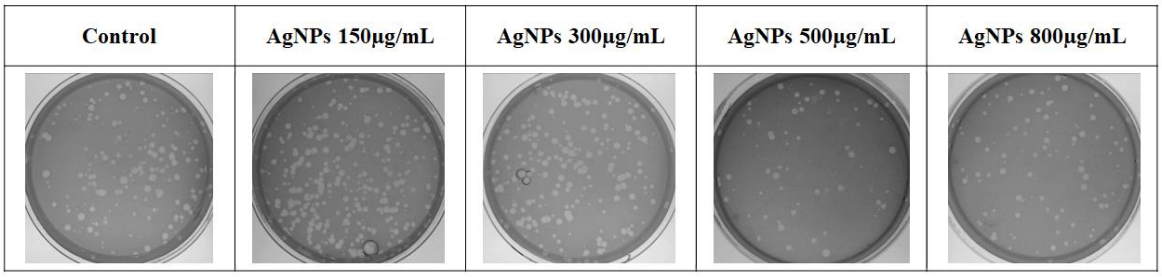

Figure 6. Bacteriophage phi 6 viability determined by the double-layer method. Titration images of undiluted samples for control and the different AuNPs concentrations at 24h of viral contact.

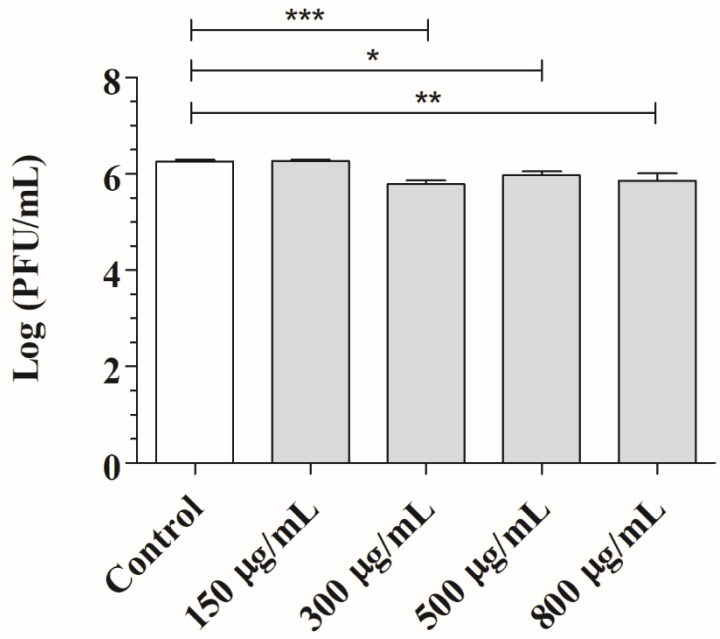

Figure 7. Reduction of infection titers of the bacteriophage phi 6 (surrogate virus of SARS-CoV-2) in logarithms of plaque-forming units per mL (log(PFU/mL)) measured by the double-layer method. Bacteriophages after being in contact with gold nanoparticles at different concentrations (150, 300, 500 and 800 µg/mL) and without being in contact (control) at 24 h of viral contact. Three independent antiviral tests were performed on two different days (n= 6). Significant differences with respect to control were determined by one-way ANOVA with Tukey's correction for multiple comparisons: ***p < 0.001; **p < 0.01; *p < 0.05; ns, not significant.

4. Discussion

The gold nanoparticles used in this study have an average size of 37.9±8.9 nm, ranging between 10 and 60 nm (see HR-TEM images in Figure 1). The Fourier Transform

was performed to index the crystalline planes of these nanoparticles (Figure 1c). The planes (400) and (200) of the AuNPs are shown with reference to the interplanar distances of 1,020 Å and 2,355 Å, respectively. Both planes refer to the cubic structure of gold, with space group *Fm-3m* (no. 225) and lattice parameter a = 4.0786 Å. This structure conforms to card no. 4-784 in the *Joint Committee on Powder Diffraction Standards* (JCPDS) database [28].

As expected, at basic pH, the effective surface charge of AuNPs was extremely negative and their surface charge becomes more positive as pH increases (Figure 1d). The isoelectric point of these particles is around pH 4 through the projection of the curve of measurements of ζ as a function of pH.

As expected, the particle size values (Table 1) show that the size values depend on the nanofluid used [29]. The PdI values of the samples were also measured by this technique to provide a particle aggregation parameter. The AuNPs showed PdI values slightly higher in DMEM than in water, which could be attributed to the higher aggregation of nanoparticles in this media, which could also explain the increase in of DLS size with respect to that measured in water.

AuNP cytotoxicity in human HaCaT cells is time-dependent, since a concentration of up to 300 µg/mL did not show any *in vitro* toxic effect at 3, 12 and 24 h (Figure 2). However, higher concentrations (500 and 300 µg/mL) did have some toxic effects, especially at 24 h.

None of the concentrations tested affected the survival rate (%) after 24 (acute toxicity) or 72 hours (chronic toxicity) by the *in vivo* toxicity assays using *C. elegans* (Figure 3A and 3B). The length of the nematodes was also monitored, and no statistical differences were found after 24 hours (Figure 3C) or 72 hours (Figure 3D), demonstrating that AuNPs are not toxic *in vivo* in the *C. elegans* model.

No proliferative effect (Figure 4) was found at 72 hours in the HaCat cell line at the selected concentrations (10, 20 and 40 µg/mL), despite having an effect in the cytotoxicity tests after 24 hours. It appears that this effect stops or matches the growth produced in the control group over time.

The expression levels of the different genes involved in different tissues were analyzed to determine the activation or inhibition of different metabolic routes (oxidative stress, extracellular matrix, synthesis of proteins related to the maintenance and repair of different tissues) due to the exposure of the different nanomaterials in human keratinocyte HaCaT cells. However, none of the analyzed 13 genes (*SOD1, CAT, MMP1, TGFB1, GPX1, FN1, HAS2, LAMB1, LUM, CDH1, COL4A1, FBN* and *VCAN*) had their expression modified after exposure to AuNPs at non-cytotoxic concentrations in human keratoncyte HaCaT after 24 hours. These results of gene expression are very different in comparison to other nanomaterials such as graphene oxide[30], graphene nanoplatelets[31], carbon nanofibers or silver nanoparticles[24], which did not showed this biological inactivity.

Cellular uptake of nanoparticles can be specific or nonspecific, depending on the ligand-receptor interaction [32]. Previous studies have found that this uptake and exchange increases with Au particle diameters of less than 10 nm [33]. In the case of specific uptake ligands to receptors on the cell membrane, these bind to membrane-bound transferrin receptors [34–36], conjugating with the surface of the gold particles. This specific uptake is more efficient than a nonspecific uptake, as ligand-modified Au particles are predominantly taken up by cells possessing the receptors for these ligands, but not by other cells. This is of great interest in the case of cancer cells, since these receptors are expressed to a greater extent on them than on the surface of healthy cells [37]. In the present study, when using larger diameter nanoparticles, we found that none

of the tests produced an effect derived from exposure to this material, even though its cytotoxicity was very low, since it only showed adverse effects at high concentrations and after long periods of exposure to the compound. It is thus a material of great interest for the design of medical devices and minimize interaction with tissues or cells for use as a vehicle, together with other compounds that do interact in one way or another, according to the objective desired.

Although, there are statistically significant reductions of infection titers at AuNP concentrations of from 300 to 800 μg/mL (Figure 7), these reductions are lower than 1 log unit after 24 h of viral contact, so that AuNPs can be said to have low or insignificant antiviral properties, allowing for experimental uncertainty.

The size and dispersion capacity of nanoparticles have been shown to have great relevance due to the scope of the effects produced by their exposure [38]. While sizes less than 15 nm in diameter are focused on applications linked to immunology or biochemistry, larger sizes between 80 and 250 nm are used in X-ray optics and electrical or medical applications [39]. In our case, we used nanoparticles considered to be of medium size (from 10 to 60 nm). Probably derived from this, it can be seen that this material does not cause modifications at the cellular level or in antimicrobial capacity. In this latter case, positive results have been observed using nanoparticles of sizes less than 20 nm against strains such as *E. coli, S. aureus, B. Subtilis, P. aeruginosa* or *S. epidermis* [40–44].

Conclusions

The results of this study demonstrate that gold nanoparticles (AuNPs) are highly stable inactive materials. They showed no toxicity *in vivo* at concentrations up 800 μg/mL in the *C. elegans* model, and non-toxicity (up to 300 μg/mL) in human keratinocytes. At 10, 20, and 40 μg/mL they did not have any proliferative capacity or any ability to induce gene expression on a battery of 13 genes after 24 hours of exposure. They also showed low or insignificant antiviral activity against a surrogate of SARS-CoV-2. The results thus demonstrate the extreme inactivity of AuNPs in human keratinocytes and against enveloped viruses such as SARS-CoV-2. Our research findings thus point the way to optimizing antimicrobial materials with AuNPs in biomedical and clinically relevant applications.

Funding

This research was supported by the *Fundación Universidad Católica de Valencia San Vicente Mártir*, Grant 2020-231-006UCV and by the Spanish Ministry of Science and Innovation (PID2020-119333RB-I00 / AEI / 10.13039/501100011033) (awarded to Á.S-A). J.A. is grateful to the *Universitat Jaume I* for Project UJI-B2019-30, to the *Generalitat Valenciana* for Project AICO2020, and the *Ministerio de Ciencia, Innovación y Universidades* (Spain) Project PGC2018- 094417-B-I00 for supporting this research financially. M.A. was supported by the Margarita Salas postdoctoral contract MGS/2021/21 (UP2021-021) financed by the European Union-Next Generation.

Acknowledgments

The authors would like to express their gratitude to the *Fundación Universidad Católica de Valencia San Vicente Mártir* and to the Spanish Ministry of Science and Innovation for their financial support.

Author Contributions

Á.S.-A. conceived the idea for this work; B.S., P.F.-M., A.T.-M., A.C.-V. performed the experimental biological characterization; M.A. performed the experimental physical-chemical characterization; Á.S.-A. led the work and wrote the draft manuscript; B.S., A.T.-M., A.C.-V., M.A., J.A. and Á.S.-A. edited and proof-read the manuscript. All the authors have read and agreed to the published version of the manuscript.

Competing interests

The authors do not have any conflicts of interest to declare.

Data availability

All data generated or analysed during this study are included in this published article

References

[1] Y. Chen, Y. Xianyu, X. Jiang, Surface Modification of Gold Nanoparticles with Small Molecules for Biochemical Analysis, Acc. Chem. Res. 50 (2017) 310–319. https://doi.org/10.1021/acs.accounts.6b00506.

[2] Y. Genji Srinivasulu, Q. Yao, N. Goswami, J. Xie, Interfacial engineering of gold nanoclusters for biomedical applications, Mater. Horizons. 7 (2020) 2596–2618. https://doi.org/10.1039/d0mh00827c.

[3] J. Zhang, L. Mou, X. Jiang, Surface chemistry of gold nanoparticles for health-related applications, Chem. Sci. 11 (2020) 923–936. https://doi.org/10.1039/C9SC06497D.

[4] N. Dasgupta, S. Ranjan, Nanotechnology in food sector. An Introduction to food grade nanoemulsions, 2018. http://www.springer.com/series/8380%0Ahttp://link.springer.com/10.1007/978-981-10-6986-4.

[5] X. Liu, Q. Dai, L. Austin, J. Coutts, G. Knowles, J. Zou, H. Chen, Q. Huo, A one-step homogeneous immunoassay for cancer biomarker detection using gold nanoparticle probes coupled with dynamic light scattering, J. Am. Chem. Soc. 130 (2008) 2780–2782. https://doi.org/10.1021/ja711298b.

[6] M. Turner, V.B. Golovko, O.P.H. Vaughan, P. Abdulkin, A. Berenguer-Murcia, M.S. Tikhov, B.F.G. Johnson, R.M. Lambert, Selective oxidation with dioxygen by gold nanoparticle catalysts derived from 55-atom clusters, Nature. 454 (2008) 981–983. https://doi.org/10.1038/nature07194.

[7] K. Saha, S.S. Agasti, C. Kim, X. Li, V.M. Rotello, Gold nanoparticles in chemical and biological sensing, Chem. Rev. 112 (2012) 2739–2779. https://doi.org/10.1021/cr2001178.

[8] W.C.W. Chan, Bio-Applications of Nanoparticles, Springer New York, New York, NY, 2007. https://doi.org/10.1007/978-0-387-76713-0.

[9] L.H. Fu, J. Yang, J.F. Zhu, M.G. Ma, Synthesis of gold nanoparticles and their

applications in drug delivery, in: Met. Nanoparticles Pharma, Springer International Publishing, 2017: pp. 155–191. https://doi.org/10.1007/978-3-319-63790-7_9.
[10] A. Sani, C. Cao, D. Cui, Toxicity of gold nanoparticles (AuNPs): A review, Biochem. Biophys. Reports. 26 (2021) 100991. https://doi.org/10.1016/j.bbrep.2021.100991.
[11] D.A. Giljohann, D.S. Seferos, W.L. Daniel, M.D. Massich, P.C. Patel, C.A. Mirkin, Gold nanoparticles for biology and medicine, Angew. Chemie - Int. Ed. 49 (2010) 3280–3294. https://doi.org/10.1002/anie.200904359.
[12] S. Shamaila, N. Zafar, S. Riaz, R. Sharif, J. Nazir, S. Naseem, Gold nanoparticles: An efficient antimicrobial agent against enteric bacterial human pathogen, Nanomaterials. 6 (2016) 71. https://doi.org/10.3390/nano6040071.
[13] S. Sathiyaraj, G. Suriyakala, A. Dhanesh Gandhi, R. Babujanarthanam, K.S. Almaary, T.W. Chen, K. Kaviyarasu, Biosynthesis, characterization, and antibacterial activity of gold nanoparticles, J. Infect. Public Health. 14 (2021) 1842–1847. https://doi.org/10.1016/j.jiph.2021.10.007.
[14] Y. Zhang, T.P. Shareena Dasari, H. Deng, H. Yu, Antimicrobial Activity of Gold Nanoparticles and Ionic Gold, J. Environ. Sci. Heal. - Part C Environ. Carcinog. Ecotoxicol. Rev. 33 (2015) 286–327. https://doi.org/10.1080/10590501.2015.1055161.
[15] U. Rajchakit, V. Sarojini, Recent Developments in Antimicrobial-Peptide-Conjugated Gold Nanoparticles, Bioconjug. Chem. 28 (2017) 2673–2686. https://doi.org/10.1021/acs.bioconjchem.7b00368.
[16] F. Dehghani, S. Mosleh-Shirazi, M. Shafiee, S.R. Kasaee, A.M. Amani, Antiviral and antioxidant properties of green synthesized gold nanoparticles using Glaucium flavum leaf extract, Appl. Nanosci. 13 (2023) 4395–4405. https://doi.org/10.1007/s13204-022-02705-1.
[17] A. Babaei, S.M. Mousavi, M. Ghasemi, N. Pirbonyeh, M. Soleimani, A. Moattari, Gold nanoparticles show potential in vitro antiviral and anticancer activity, Life Sci. 284 (2021) 119652. https://doi.org/10.1016/j.lfs.2021.119652.
[18] E. Paradowska, M. Studzińska, A. Jabłońska, V. Lozovski, N. Rusinchuk, I. Mukha, N. Vitiuk, Z.J. Leśnikowski, Antiviral effect of nonfunctionalized gold nanoparticles against herpes simplex virus type-1 (Hsv-1) and possible contribution of near-field interaction mechanism, Molecules. 26 (2021) 5960. https://doi.org/10.3390/molecules26195960.
[19] J. Vonnemann, C. Sieben, C. Wolff, K. Ludwig, C. Böttcher, A. Herrmann, R. Haag, Virus inhibition induced by polyvalent nanoparticles of different sizes, Nanoscale. 6 (2014) 2353–2360. https://doi.org/10.1039/c3nr04449a.
[20] A.M. Paul, Y. Shi, D. Acharya, J.R. Douglas, A. Cooley, J.F. Anderson, F. Huang, F. Bai, Delivery of antiviral small interfering RNA with gold nanoparticles inhibits dengue virus infection in vitro, J. Gen. Virol. 95 (2014) 1712–1722. https://doi.org/10.1099/vir.0.066084-0.
[21] D. Baltimore, Expression of animal virus genomes., Bacteriol. Rev. 35 (1971) 235–241. https://doi.org/10.1128/mmbr.35.3.235-241.1971.
[22] A. Cano-Vicent, A. Tuñón-Molina, M. Martí, Y. Muramoto, T. Noda, K. Takayama, Á. Serrano-Aroca, Antiviral face mask functionalized with solidified hand soap: low-cost infection prevention clothing against enveloped viruses such as SARS-CoV-2, ACS Omega. (2021). https://doi.org/https://doi.org/10.1021/acsomega.1c03511.
[23] Á. Serrano-Aroca, Antiviral Characterization of Advanced Materials: Use of

Bacteriophage Phi 6 as Surrogate of Enveloped Viruses Such as SARS-CoV-2, Int. J. Mol. Sci. 2022, Vol. 23, Page 5335. 23 (2022) 5335. https://doi.org/10.3390/IJMS23105335.
[24] B. Salesa, M. Assis, J. Andrés, Á. Serrano-Aroca, Carbon Nanofibers versus Silver Nanoparticles: Time-Dependent Cytotoxicity, Proliferation, and Gene Expression, Biomedicines. 9 (2021) 1155. https://doi.org/10.3390/biomedicines9091155.
[25] A. Tuñón-Molina, M. Martí, Y. Muramoto, T. Noda, K. Takayama, Á. Serrano-Aroca, Antimicrobial Face Shield: Next Generation of Facial Protective Equipment against SARS-CoV-2 and Multidrug-Resistant Bacteria, Int. J. Mol. Sci. 2021, Vol. 22, Page 9518. 22 (2021) 9518. https://doi.org/10.3390/IJMS22179518.
[26] M. Martí, A. Tuñón-Molina, F.L. Aachmann, Y. Muramoto, T. Noda, K. Takayama, Á. Serrano-Aroca, Protective Face Mask Filter Capable of Inactivating SARS-CoV-2, and Methicillin-Resistant Staphylococcus aureus and Staphylococcus epidermidis, Polymers (Basel). 13 (2021) 207. https://doi.org/10.3390/polym13020207.
[27] A.M. Kropinski, A. Mazzocco, T.E. Waddell, E. Lingohr, R.P. Johnson, Enumeration of bacteriophages by double agar overlay plaque assay., Methods Mol. Biol. 501 (2009) 69–76. https://doi.org/10.1007/978-1-60327-164-6_7.
[28] M.R. Bindhu, M. Umadevi, Antibacterial activities of green synthesized gold nanoparticles, Mater. Lett. 120 (2014) 122–125. https://doi.org/10.1016/j.matlet.2014.01.108.
[29] T. Aguilar, E. Sani, L. Mercatelli, I. Carrillo-Berdugo, E. Torres, J. Navas, Exfoliated graphene oxide-based nanofluids with enhanced thermal and optical properties for solar collectors in concentrating solar power, J. Mol. Liq. 306 (2020) 112862. https://doi.org/10.1016/j.molliq.2020.112862.
[30] B. Salesa, Á. Serrano-Aroca, Multi-Layer Graphene Oxide in Human Keratinocytes: Time-Dependent Cytotoxicity, Proliferation, and Gene Expression, Coatings. 11 (2021) 414. https://doi.org/10.3390/coatings11040414.
[31] B. Salesa, A. Tuñón-Molina, A. Cano-Vicent, M. Assis, J. Andrés, Á. Serrano-Aroca, Graphene Nanoplatelets: In Vivo and In Vitro Toxicity, Cell Proliferative Activity, and Cell Gene Expression, Appl. Sci. 2022, Vol. 12, Page 720. 12 (2022) 720. https://doi.org/10.3390/APP12020720.
[32] B.D. Chithrani, A.A. Ghazani, W.C.W. Chan, Determining the size and shape dependence of gold nanoparticle uptake into mammalian cells, Nano Lett. 6 (2006) 662–668. https://doi.org/10.1021/nl052396o.
[33] R.A. Sperling, P.R. Gil, F. Zhang, M. Zanella, W.J. Parak, Biological applications of gold nanoparticles, Chem. Soc. Rev. 37 (2008) 1896–1908. https://doi.org/10.1039/b712170a.
[34] E. Wagner, D. Curiel, M. Cotten, Delivery of drugs, proteins and genes into cells using transferrin as a ligand for receptor-mediated endocytosis, Adv. Drug Deliv. Rev. 14 (1994) 113–135. https://doi.org/10.1016/0169-409X(94)90008-6.
[35] P.H. Yang, X. Sun, J.F. Chiu, H. Sun, Q.Y. He, Transferrin-mediated gold nanoparticle cellular uptake, Bioconjug. Chem. 16 (2005) 494–496. https://doi.org/10.1021/bc049775d.
[36] V. Dixit, J. Van Den Bossche, D.M. Sherman, D.H. Thompson, R.P. Andres, Synthesis and grafting of thioctic acid-PEG-folate conjugates onto Au nanoparticles for selective targeting of folate receptor-positive tumor cells, Bioconjug. Chem. 17 (2006) 603–609. https://doi.org/10.1021/bc050335b.

[37] P.K. Jain, I.H. ElSayed, M.A. El-Sayed, Au nanoparticles target cancer, Nano Today. 2 (2007) 18–29. https://doi.org/10.1016/S1748-0132(07)70016-6.
[38] X. Gu, Z. Xu, L. Gu, H. Xu, F. Han, B. Chen, X. Pan, Preparation and antibacterial properties of gold nanoparticles: a review, Environ. Chem. Lett. 19 (2021) 167–187. https://doi.org/10.1007/s10311-020-01071-0.
[39] M. Shah, V. Badwaik, Y. Kherde, H.K. Waghwani, T. Modi, Z.P. Aguilar, H. Rodgers, W. Hamilton, T. Marutharaj, C. Webb, M.B. Lawrenz, R. Dakshinamurthy, Gold nanoparticles: Various methods of synthesis and antibacterial applications, Front. Biosci. - Landmark. 19 (2014) 1320–1344. https://doi.org/10.2741/4284.
[40] N. Abdel-Raouf, N.M. Al-Enazi, I.B.M. Ibraheem, Green biosynthesis of gold nanoparticles using Galaxaura elongata and characterization of their antibacterial activity, Arab. J. Chem. 10 (2017) S3029–S3039. https://doi.org/10.1016/j.arabjc.2013.11.044.
[41] L.T. Lanh, T.T. Hoa, N.D. Cuong, D.Q. Khieu, D.T. Quang, N. Van Duy, N.D. Hoa, N. Van Hieu, Shape and size controlled synthesis of Au nanorods: H2S gas-sensing characterizations and antibacterial application, J. Alloys Compd. 635 (2015) 265–271. https://doi.org/10.1016/j.jallcom.2015.02.146.
[42] K.D. Lee, P.C. Nagajyothi, T.V.M. Sreekanth, S. Park, Eco-friendly synthesis of gold nanoparticles (AuNPs) using Inonotus obliquus and their antibacterial, antioxidant and cytotoxic activities, J. Ind. Eng. Chem. 26 (2015) 67–72. https://doi.org/10.1016/j.jiec.2014.11.016.
[43] S. Vanaraj, J. Jabastin, S. Sathiskumar, K. Preethi, Production and Characterization of Bio-AuNPs to Induce Synergistic Effect Against Multidrug Resistant Bacterial Biofilm, J. Clust. Sci. 28 (2017) 227–244. https://doi.org/10.1007/s10876-016-1081-0.
[44] P. Boomi, G.P. Poorani, S. Selvam, S. Palanisamy, S. Jegatheeswaran, K. Anand, C. Balakumar, K. Premkumar, H.G. Prabu, Green biosynthesis of gold nanoparticles using Croton sparsiflorus leaves extract and evaluation of UV protection, antibacterial and anticancer applications, Appl. Organomet. Chem. 34 (2020) e5574. https://doi.org/10.1002/aoc.5574.